biological tissues. The set up, makes use of super luminescent diode sources with center wavelengths of ~ 840nm and ~ 1305nm. The diode output was coupled into a fiber optic based Michelson interferometer by use of a 3-dB bi-directional fused fiber coupler designed for the wavelength used. The light beam in the sample arm was collimated and focused on to the sample with a microscopic objective.

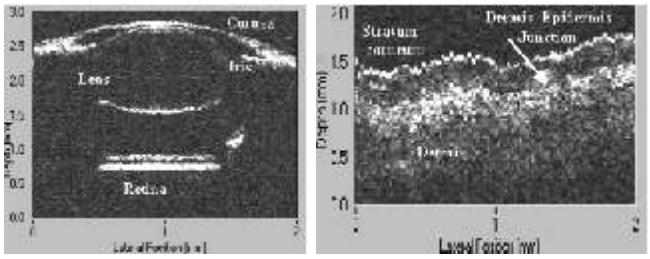

(a) (b)

Fig L.6.1 *(a) Image of fish eye showing different layers (b) In-vivo image of human skin (finger-pad)*

The reference mirror was mounted on a linear translation stage and translated back and forth with a uniform velocity. The light reflected from both the sample and reference arms was detected by a photodiode and the resulting interferogram was demodulated using a lock-in amplifier. The interferogram envelope was digitized and acquired in a PC using a data acquisition card. Lateral scanning was done using a stepper motor. The axial and lateral resolutions of the setup in free space were ~11mm and 27mm respectively at 840 nm and ~25ìm and 40ìm respectively at 1305mm. The image of a fish eye acquired with the 1305nm set up is shown in fig. L.6.1(a). The different layers of the eye like the cornea, iris, lens and the retina can be clearly seen. The set up has also been used for in–vivo imaging of human skin (fig. (b)). The stratum corneum and the epidermis-dermis junction are clearly visible. Real time imaging set up using a rapid scanning optical delay line is being assembled and should prove useful for dermatological applications.

(Contributed by: K Divakar Rao and P. K. Gupta: pkgupta@cat.ernet.in)

L.7 Interaction dynamics of RBC in optical tweezers : prospects for microfluidic actuations and diagnosis of malaria

There exists considerable current interest in understanding the interaction of objects of different shape with the trap beam in an optical tweezers set up. Apart from furthering basic understanding of trapping forces such interactions can also be used for construction of micromotors and other devices. Red blood cells provide a good model system for this purpose because their shape can be conveninetly modulated by a change in the osmolarity of the suspension in which these are placed. We have investigated the dynamics of the interaction of RBC with trap laser beam at different osmolarity of the suspension and power of the trap beam. RBCs suspended in isotonic buffer (~300 mOsm/kg) are discotic and when optically tweezed they reorient and align with their edge length along the trap laser propagation direction. The time required for a RBC to switch from initial horizontal position to the vertical orientation was found to decrease with both an increase in the trapping power and osmolarity of the buffer. At 85 mW trap beam power the time required varied from 240 ms to 120 ms for a change in osmolarity from 300 mOsm/Kg to 800 mOsm/Kg. The vertically oriented RBCs take a longer time to return to the horizontal orientation when the trap beam is put off. Faster reorientation to horizontal plane (~ 0.2 s) could be achieved by subjecting the RBC to a burst of radiation pressure from a focused pulsed laser or to a viscous drag on its surface closer to the cover slip by translation of the microscope stage. These experiments also showed that contrary to a recent report there does not occur any folding of the RBC membrane when it is optically tweezed. The switching of RBC from horizontal to vertical plane or vice-versa can be utilized as an optically controlled valve. For this application use of a linearly polarized trap beam offers an added advantage because then the RBC orients with its plane oriented along the plane of polarization of the trapping beam. By rotating the plane of polarization of the trap beam the disk can be oriented at different angles about the trap beam axis.

More interestingly, we found [S. K. Mohanty, A. Uppal, P. K. Gupta, *Biotechnol. Lett.* 26, 971-974 (2004)] that in hypertonic buffer medium (osmolarity > 800mOsm/kg), the meniscus shaped normal RBC rotates when optically trapped with trap beam power beyond ~ 40mW (fig.L.7.1). This arises due to the torque generated on the cell by transfer of linear momentum from the trapping beam. For a given osmolarity the rotational speed was observed to increase super-linearly with an increase in trap beam power. RBC having malaria parasite in it (as confirmed by fluorescence of acridine orange stain) does not rotate. Even more significant is the fact that the rotational speed of other RBCs from malaria-infected blood sample, which did not show acridine orange fluorescence, was an order of magnitude smaller and increased much slower with an increase in trap beam power as compared to normal cells. We could screen around 40 RBCs/min by making the cells flow through the trapping point at a velocity of ~ 10 mm/sec. When a flowing RBC struck a trapped RBC, the trapped RBC was thrown out by the collision and the other RBC gets trapped and starts rotating if normal. Higher-screening rates are possible by increasing the flow rate of RBCs and by increasing the number of traps in an array

orthogonal to the direction of flow. This approach can provide higher throughput and sensitivity of detection of malaria as compared to the current frontline approaches and can also be used for diagnosis of other diseases that results in changes in the elasticity of RBC membrane, like leukemia.

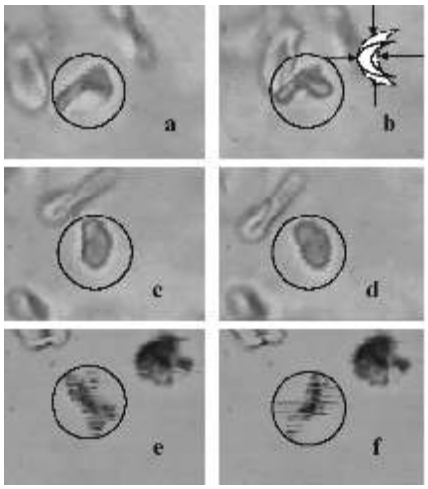

Fig. L.7.1 Rotation of a normal RBC trapped by optical tweezers. The cell (encircled) was suspended in a hypertonic buffer and trapped at power levels that varied from (a) 40 mW to (b) 200 mW. Figure 1(b) inset shows a schematic of the deformation observed in the horizontal cross section of a RBC structure at a higher trap beam power (solid curve). The dotted curve corresponds to the shape observed without the trapping beam. Arrows illustrate the transverse gradient force of optical tweezers. (c) and (d) show time-lapsed digitized video images of RBC rotation at a buffer osmolarity of 1,000 mOsm/kg; images in (e) and (f) represent an osmolarity of 1,250 mOsm/kg. The trap power was 80 mW and the time lapse between consecutive frames was 80 ms. The speed of rotation was estimated to be 25 rpm at 1,000 mOsm/kg and 200 rpm at 1,250 mOsm/kg.

(Contributed by: S.K Mohanty, A. Uppal,
P. K. Gupta: pkgupta@cat.ernet.in)

L.8 Rotation of transparent, non-birefringent objects by transfer of optical spin angular momentum

Transfer of light angular momentum to trapped objects is being actively investigated both from the point of view of fundamental understanding of the process and the potential of this transfer for realization of all optically driven micro machines. Control of rotation speed in optically driven micro machines using orbital angular momentum transfer requires a change in the power of trapping beam which may not be desirable because of possible adverse effects on the rotating object(s) at higher power levels. In this respect optically driven micro machines using transfer of light spin angular momentum have the advantage in that their rotation speed can be controlled by a control on ellipticity of the trap beam. However, so far transfer of spin angular momentum of light has been reported only for those cases where the object is birefringent or absorbing. Transfer of spin angular momentum should also occur if the incident and emerging rays are in different directions. An angular momentum equal and opposite of the vector difference between the spin angular momentum of the emergent and incident rays should act on the trapped object. For the case of a spherically symmetric objects, trapped in equilibrium position with its center coincident with geometrical focus of trapping beam there is no change in the direction of the trapping rays and hence there is no transfer of angular momentum. It is perhaps for this reason that transfer of spin angular momentum to transparent non-birefringent objects was not attempted.

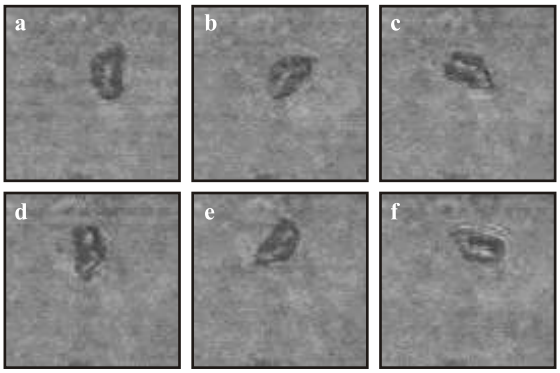

Fig L.8.1 *Digitized time laps images of rotating $NaBrO_3$ crystal*

We analyzed propagation of elliptically polarized light through isotropic objects of different shapes trapped in equilibrium configuration and found that the change in the direction of the incident and the refracted rays is particularly significant in case of a tetrahedral shaped object. Therefore, to demonstrate the effect we selected an isotropic tetrahedral crystal i.e. sodium bromate. We selected 1-octanol (η_o=1.428) as the surrounding medium because it has a lower index of refraction compared to sodium bromate, no chemical reactivity with sodium bromate and its high viscosity (η_o=10.6 cP) prevents the small sodium bromate crystals (specific gravity = 3.39) from settling down quickly on the cover glass and get attached to the surface by strong Van der Waals force. In order to observe the rotation of this crystal by transfer of spin angular momentum from the trapping beam we used a conventional laser tweezers set up. For trapping beam power of ~ 32mW at the specimen plane the experimentally observed rotational frequency was 0.21 Hz in reasonable agreement with our estimates (Fig. L.8.1). In fig. L.8.2 we show the change affected in the rotational speed of the trapped object by a change in the ellipticity of polarization